High Energy Solar Physics: Anticipating HESSI
ASP Conference Series, Vol. xxx, 2000
R. Ramaty and N. Mandzhavidze, eds.

The HESSI Spectrometer

D. M. Smith, R. P. Lin, P. Turin, D. W. Curtis, J. H. Primbsch, R. D. Campbell, R. Abiad

Space Sciences Laboratory, U. C. Berkeley, Berkeley, CA 94720

C. Cork, E. Hull, D. Landis, N. W. Madden, D. Malone, R. Pehl

Lawrence Berkeley National Laboratory

R. Schwartz

NASA Goddard Space Flight Center/Raytheon STX

Abstract. HESSI will perform spectroscopy from roughly 3 keV to 17 MeV, well over three orders of magnitude in energy, with a single set of 9 cryogenically cooled germanium detectors. Here we describe the HESSI spectrometer, discuss the procedures for spectroscopic data analysis, and show the estimated sensitivity of HESSI to important features of flare spectra.

1. Introduction

The HESSI spectrometer design was driven by the need to satisfy many requirements with a single instrument of modest cost and weight. The spectrometer had to be able to process tens-to-hundreds of thousands of hard x-rays per second for imaging, while carefully collecting rare gamma-ray line photons with high efficeny, high energy resolution, and without interference from the x-rays. The energy range had to extend down to 3 or 4 keV to clearly image the thermal components of flares and to be highly sensitive to microflares, while extending well above the 4.4 and 6.1 MeV gamma-ray lines to characterize the electron bremsstrahlung spectrum above the nuclear line region. We wanted to be sensitive to events covering at least seven orders of magnitude in intensity, from microflares to the largest X-class events.

2. The HESSI germanium detectors

To meet all these goals within the cost and weight constraints of a Small Explorer mission, we designed an array of segmented coaxial germanium detectors. Ultrapure germanium at cryogenic temperatures is an insulator, but a hard x-ray or gamma ray interacting in the crystal will release one or more energetic electrons, which lose energy by creating free electron-hole pairs. If there is a high electric field (on the order of 1000 V/cm) across the crystal, the electrons

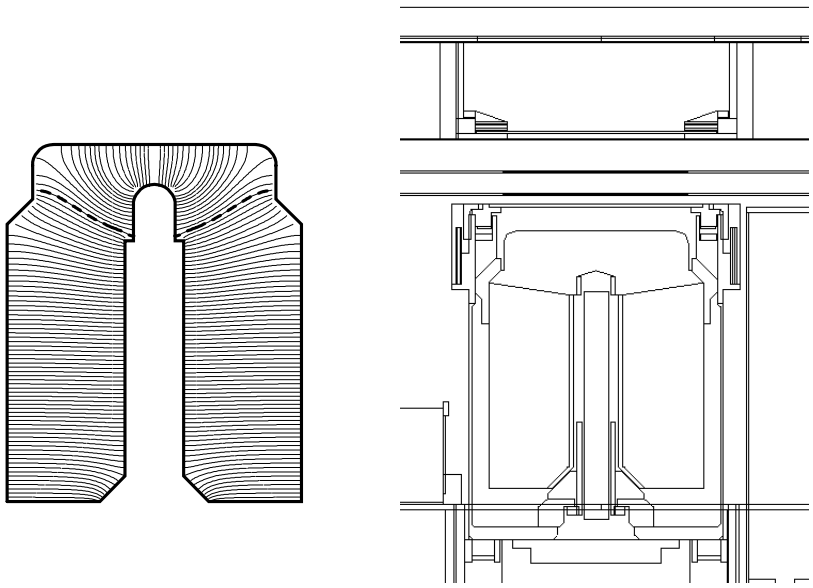

Figure 1. Cross-sections of a HESSI detector. Left: a detector profile with field lines, with the field line marking the segment boundary in bold dashes. Right: a detector in the cryostat, showing Ta/Sn/Fe/Al shielding around the side of the front segment and above the shoulder of the rear segment.

and holes will be pulled to each electrode, creating a current pulse which can be amplified and digitized by suitable electronics. The total charge in the current pulse is proportionate to the photon energy. At low energies (below about 200 keV) the width of a spectral line is dominated by noise in the electronics, and is roughly constant; above 200 keV it is dominated by the counting statistics of the electron-hole pairs, and increases roughly as the square root of energy (so that the resolution, $E/\Delta E$, improves with energy).

Figure 1 shows two cross-sections of the cylindrically-symmetrical HESSI detector design. This design was a joint effort of the HESSI co-investigators at U. C. Berkeley and Lawrence Berkeley National Laboratory and the manufacturer, PerkinElmer Instruments. The shape is a variation of a "closed-end coaxial" detector, the industry standard design for large volumes and high gamma-ray sensitivity. Two conductive layers are implanted on the crystal surfaces to serve as electrodes: a thin, p-type layer of implanted boron on the front and side surfaces, and a thicker, n-type layer of diffused lithium ions on the inner bore. The rear surface is left as an insulator. The material overall is very slightly n-type, and when 2000-4000V is applied between the inner and outer electrodes the crystal is depleted of these charge carriers, with enough electric field in the crystal from the space charge and external voltage to cause the electron-hole pairs to reach terminal velocity.

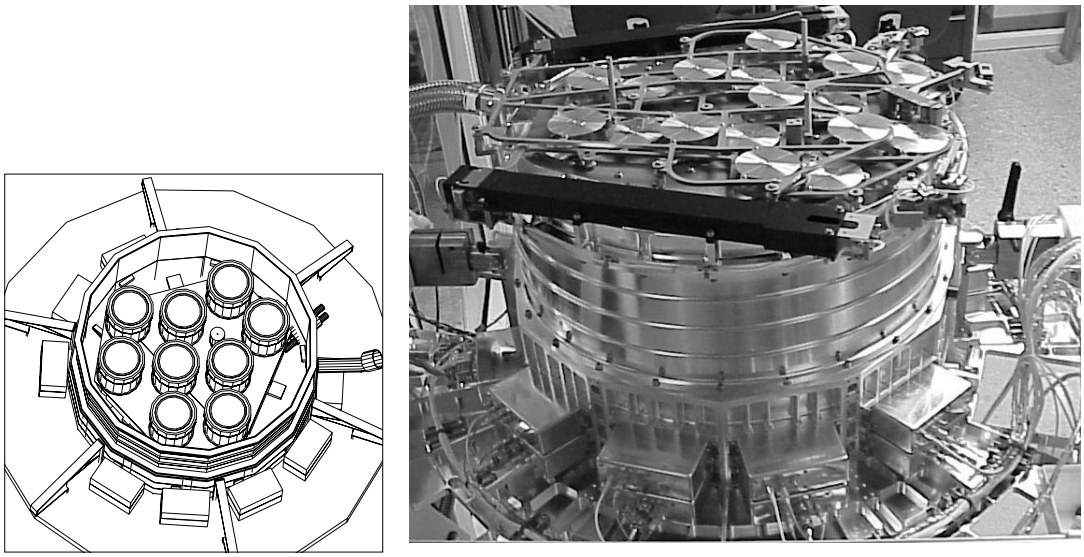

Figure 2. Left: arrangement of the HESSI detectors inside the cryostat. The small cylinder nestled among the detectors is the beryllium scatterer for polarization measurements. Right: the assembled spectrometer, showing the aluminum attenuator disks on top (one set in the aperture, the other out).

The step seen near the top of the inner bore in Figure 1 (left) is an interruption in the lithium contact. The signals are extracted separately from the two halves of this electrode. The line extending from this step to the outside edge of the detector represents a boundary electric field line: photons stopping above this line are detected in the front channel, and those stopping below it in the rear channel. Thus a single crystal becomes a stacked pair of detectors. The front segment will absorb all the hard x-rays up to about 100 keV, letting most gamma-ray line photons through. The rear segment will stop many of the latter, so that fine spectroscopy can be done without high deadtime from the x-rays.

The notch on the outer edge of the detector serves two purposes: first, it concentrates the electric field lines at the corner of the notch, so that the field line which originates at the inner step always hits the proper place on the outside of the detector. In addition, it removes some mass from in front of the rear segment, so that fewer high-energy gamma rays Compton scatter before entering the rear. To keep the "shoulder" part of the rear segment from being swamped with flare hard x-rays, a ring of thin "graded-Z" passive shielding is placed above the shoulder (Figure 1, right; also see below). This shield is just as effective as the front segment in photoelectrically absorbing hard x-rays, but with much less Compton scattering of gamma-rays.

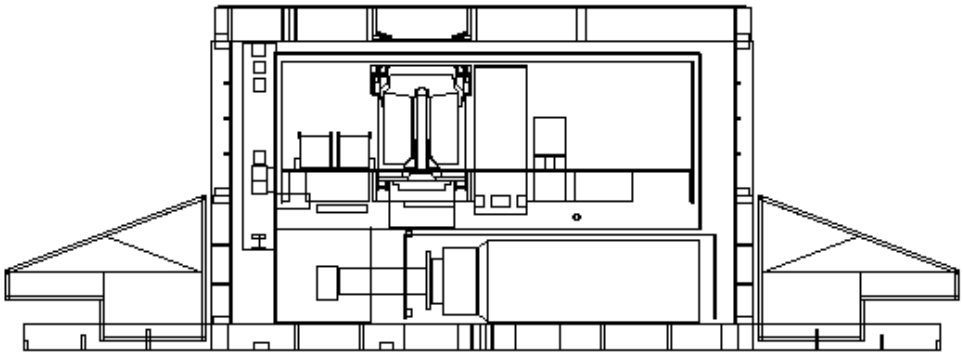

Figure 3. Side view cross-section of the spectrometer, showing the Sunpower M77 cryocooler below the coldplate, and the large-area radiatior at the bottom.

The preamplifiers for the HESSI detectors feature 4-terminal FETS with adjustable back-gate voltage for very-low-noise operation. These are immediately behind the detectors. Their signals are taken out to the rest of the preamplifier circuits, which reside in small boxes clustered around the bottom of the spectrometer (see Figure 2, right), by a harness consisting of thin traces of manganin (for low thermal conductivity) layered in a flexible plastic film. The preamplifiers use a pulsed reset circuit developed at Lawrence Berkeley National Laboratory (Landis et al. 1981). The signals from the preamplifier are taken to a signal-processing board elsewhere on the spacecraft. Each board contains both the analog and digital signal-processing circuitry for both segments of one detector. The signal from each event is split, going to a fast-shaping channel for pileup rejection and the fast-rates data (see below), and to a slow-shaping channel (8 μs) for spectroscopy.

3. The HESSI cryostat

The HESSI cryostat was designed to provide a lightweight but secure environment for the detectors. This involves maintaining a hard vacuum and very good thermal insulation, so that the detectors can remain at operating temperature (about 80K) with a very low heat leak. Figure 2 (left) depicts the interior of the cryostat and the arrangement of the detectors.

The weight constraints of a Small Explorer did not allow a heavy shield to veto solar photons which scatter out of the detectors and to keep out background photons. We therefore decided instead to design the side walls of the cryostat to be as thin as possible. This allows hard x-rays (above about 25 keV) and gamma-rays from cosmic sources such as supernova remnants, pulsars, and gamma-ray bursters to enter the spectrometer, providing a wealth of secondary science (Smith et al. 2000). Since all these sources are orders of magnitude fainter than most solar flares, and also appear primarily in the rear segments rather than

the fronts, they don't interfere with solar observations. Thin rings of passive shielding surround the side of each front segment to block hard x-rays from the cosmic diffuse background and the Earth's atmosphere. The material is a laminate of tantalum, tin, steel, and aluminum. In this "graded-Z" construction, each metal absorbs the K-shell x-rays from the one before it.

The detectors are cooled by a Sunpower model M77 Stirling cycle refrigerator, a very small, high-efficiency unit modified for long-term use in orbit by the cryogenics group of Dr. Stephen Castles at NASA's Goddard Space Flight Center. The cooler is coupled to the coldplate and detectors, which are suspended by fiberglass straps from the rest of the cryostat for thermal isolation. The coldplate assembly is surrounded by multilayer aluminized-mylar insulation and a thin aluminum thermal shield held at an intermediate temperature (about 170 K). More insulation separates the intermediate shield from the external walls at room temperature. This allows the detectors to be cooled to about 80 K with only 4W of cooling, which requires an input power of about 70W to the M77. Waste heat from the cooler is radiated to space from the back surface of the spectrometer, which is also the rearmost surface of the spacecraft. The cooler is visible in Figure 3 as the horizontal cylindrical object in the cavity below the detector area.

Attached to the top of the spectrometer are two lightweight, moveable frames, each of which carries nine aluminum disks which can be moved in front of the detectors (see Figure 2, right). These serve as attenuators, to keep the detectors from being saturated at high counting rates. The onboard computer will monitor the rates and put the disks in and out so that the deadtime remains below about 50%. One set of disks is thicker than the other, but they are not uniform: each has a small, thin spot in the center so that there is always some low-energy response. There is also a slightly larger region which is thick on the otherwise thin disk and thin on the otherwise thick disk: thus, the full attenuation doesn't occur until both disks are in place. Figure 4 (right panel) shows the attenuation caused by the thermal blankets and beryllium windows above the detectors (top trace) and the attenuation with the thin, thick, and combined attenuators. This system adds about four orders of magnitude to the dynamic range of microflares and flares detectable by HESSI.

Since the rear segments see no direct flare photons below 100 keV, we can use them at these low energies as a crude hard x-ray polarimeter. There is a cylinder of beryllium 3 cm in diameter and 3.5 cm long nestled among the rear segments (it is almost equally close to 4 of them; see Figure 2, left). Above this cylinder is a thin spot in the spectrometer shell and a hole in the grid trays, so that solar photons > 20 keV can reach the cylinder and scatter into the adjacent rear segments. The Compton cross section, differential in azimuth angle, is a function of the angle from the polarization axis. Thus, by watching the relative rates of these rear segments, we will measure the direction and degree of polarization for incoming photons of roughly 20-100 keV. Simulations show that we will be able to detect polarization fractions as low as a few percent for the largest flares. The key difficulty in the analysis will be photons scattered from the Earth's atmosphere, which also produce low-energy counts in the rears and which also vary with the spacecraft spin.

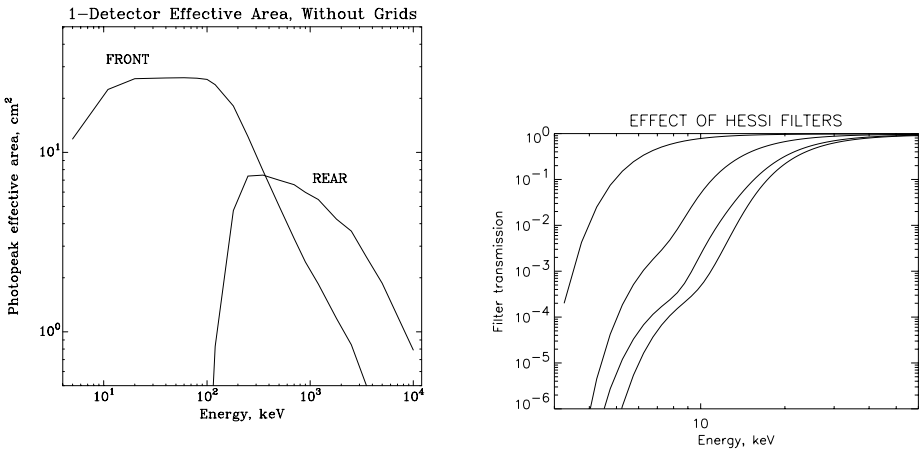

Figure 4. Left: Effective area of the front and rear segments of a single HESSI detector for photopeak detection of a downward-incident photon, without the shadowing of the grids. Right: Attenuation factor of the attenuator configurations as a function of energy.

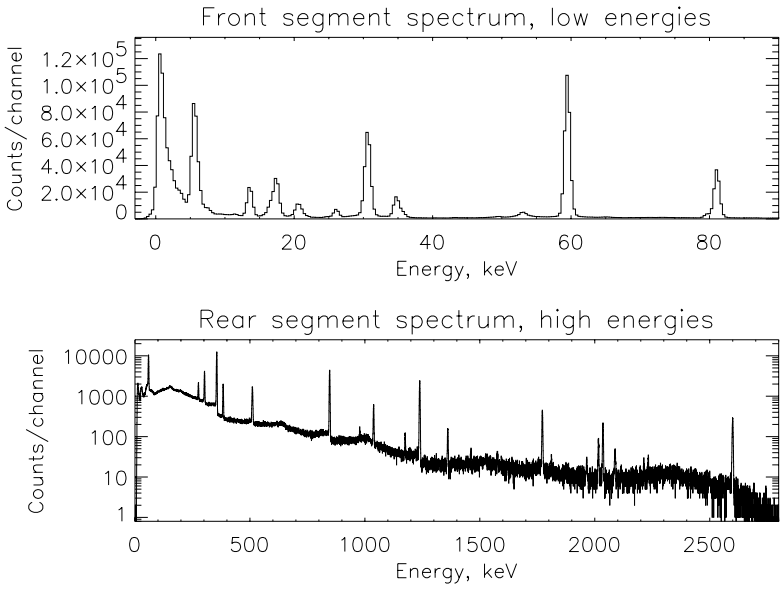

Figure 5. Front and rear segment spectra from one HESSI detector combining ^{55}Fe, ^{241}Am, ^{133}Ba, and ^{56}Co.

Line Energy (MeV)	Excited Nucleus	Width (keV)	3σ Line Fluence (ph/cm²))	Large Flare			
				Line Fluence (ph/cm²)	HESSI Line Counts	HESSI Continuum Counts *	Number of σ
Prompt lines							
0.339	^{59}Ni	4	1.6	9.2	1512	37475	7.7
0.429†	^{7}Li	5	2.4	9.5	838	15839	6.5
0.478†	^{7}Be	10	3.5	9.5	854	25342	5.3
0.452†	^{7}Li-^{7}Be	30	2.3	19.0	3195	89004	10.5
0.847	^{56}Fe	5	1.4	17.3	1074	4471	14.4
0.932	^{55}Fe	5	1.2	2.5	274	3193	4.7
1.369	^{24}Mg	16	1.7	25.5	1567	6995	16.9
1.634	^{20}Ne	20	1.6	75.3	4297	6863	40.7
1.778	^{28}Si	20	1.9	30.4	1446	5245	17.7
2.618	^{20}Ne	60	3.5	11.4	445	4187	6.5
4.439	^{12}C	145	6.9	73.3	1294	5383	15.8
6.129	^{16}O	145	11.4	57.6	549	2716	9.6
Delayed lines							
0.511	e^+/e^-	5	2.4	196.9	21060	15432	110.2
2.223	^{2}H	2.5	0.6	298.7	13345	346	114.1

* For most lines, about 90% flare continuum and 10% instrumental background for this bright flare.

† The narrow lines are for a downward beam or a fan beam; the single broad line at ~0.45 MeV is for an isotropic distribution.
This line has an intrinsic width of ~0.1 keV, so we used the instrument FWHM resolution (2.5 keV).

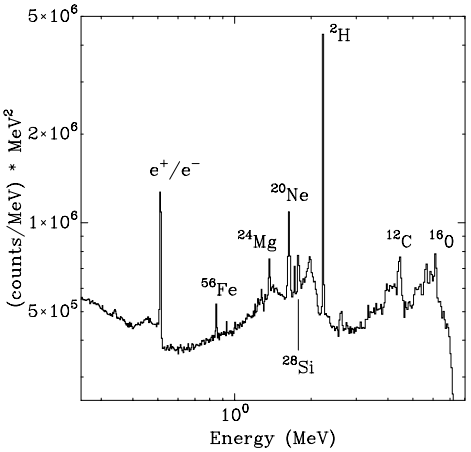

Figure 6. Left: expected sensitivities to the principal gamma-ray lines in a large flare. Right: simulated HESSI count spectrum from a large gamma-ray line flare.

4. Performance

The effective areas of single HESSI front and rear detector segments are shown in Figure 4 (left), taken from a simulation with an accuracy of a few percent. Figure 5 shows a spectrum from each segment taken with a typical HESSI detector in the laboratory. The energy resolution (FWHM) is about 920 eV in the front segment and 2.75 keV in the rear. The 5.9 keV line from ^{55}Fe can be seen toward the bottom of the front-segment spectrum. The noise counts below this line (at about 3 keV) are pulses induced by the moving charges of a large event in the rear. They can be easily removed by the data analysis software without affecting real 3 keV events, which won't be simultaneous with a rear event.

Combined with an estimate of the predicted background level, the effective area and resolution data allow us to calculate HESSI's sensitivity to the gamma-ray lines in flares. Even though HESSI carries no shielding to block background photons from the Earth or the cosmic diffuse sky, the flares which will show gamma-ray lines are so bright that the bremsstrahlung emission from the flare

itself will overwhelm these sources of background, and will therefore define the continuum above which the lines must be detected.

Figure 6 (right) shows the expected HESSI response to a bright gamma-ray line flare, with the origin of many of the lines labeled. Table 1 shows the expected sensitivity to these and other lines, defined in two ways: the statistical significance of each line for the largest expected gamma-ray line flare, and the line flux required for a 3σ detection.

The dynamic range of the detectors (without the attenuators) ranges from a few counts/s/detector (limited by background) to 26,000 counts/s/detector (limited by the response time of the signal electronics. Each photon's data are telemetered to the ground, regardless of whether a flare is in progress; no triggering on flares is required, although the count rate is monitored for the attenuators. In a special "fast rates" mode, the detectors can count nearly an order of magnitude faster for imaging with very limited spectral information: the output is the count rate vs. time in several broad energy channels. This data format is turned on if the front segment deadtime exceeds about 50%, without stopping collection of individual photons.

A major performance issue for germanium detectors in space is radiation damage, which causes trapping of the moving holes liberated by each gamma-ray photon (the electrons are relatively immune). HESSI's orbit grazes the inner edge of the proton belt a few times a day at the South Atlantic Anomaly. The damage effect is minimized in several ways. First, the configuration of the electrodes means that the holes travel to the outer electrode. Since most of the detector volume is at large radii, most photons therefore suffer relatively little hole trapping, since the holes cross relatively little damaged germanium. Second, we will keep the detectors very cold (80K), even though they can operate at much higher temperatures (up to 110K or higher). The degree of trapping produced by a given radiation dose is a strong function of temperature (Hull 1998; Koenen et al. 1995). Finally, we have heaters in the cryostat which can bring the array to 100°C; annealing for about a day at this temperature should remove all the accumulated radiation damage. From our estimate of the proton dose on orbit, we expect to anneal after a period of one to two years.

5. Spectral data analysis

Figure 7 is a block diagram of the data analysis process for HESSI spectra. The HESSI data analysis software will, like the data, be made public immediately, and should be able to bring users who don't have a detailed knowledge of the instrument to the "dotted line" in the figure: a spectrum in photons/cm^2/s/keV with all instrumental effects removed as completely as possible.

The first stage is to correct for gain drift, deadtime, and pileup of nearly simultaneous photons. Gain will be very well known, since there will be many narrow, easily identified background lines. With the two attenuators in operation, we should very seldom exceed 50% dead time, so the deadtime and pileup corrections should remain simple.

The next task is to identify and subtract background. For most flares, the user will be prompted to select the time just before and after the flare to use

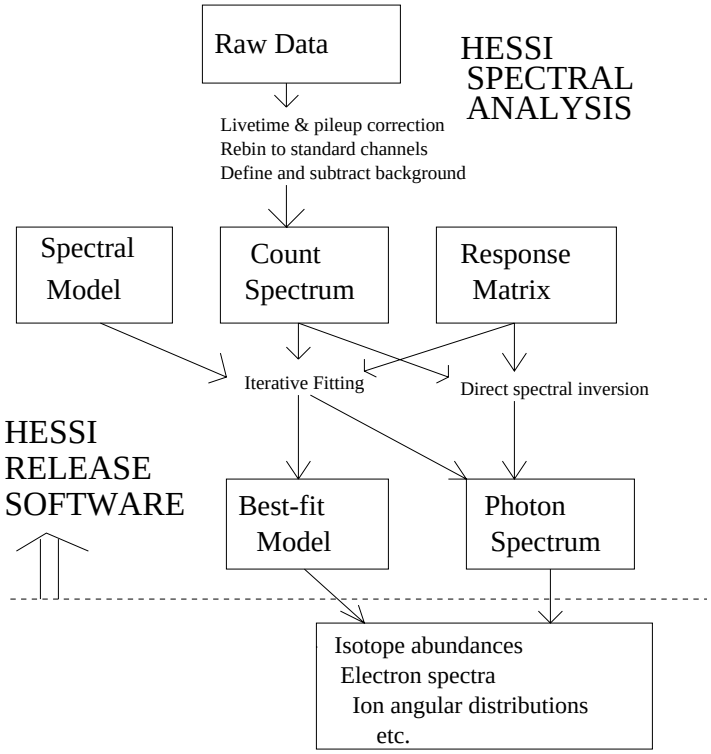

Figure 7. Diagram of the HESSI spectral analysis process.

as background time. For very long flares, the background might be selected one orbit or even one day before and after the event.

To convert a background-subtracted count spectrum to a photon spectrum, the response of the instrument must be removed. There are many effects that modify the input spectrum: absorption in the mylar blankets, cryostat windows, and grids; Compton scattering into and out of the detectors; Compton scattering from the Earth's atmosphere (which will dominate the count rate in the rear segments below 100 keV), noise in the electronics, resolution degradation due to radiation damage, the low-energy cutoff imposed by the electronics, etc. All of these effects will be accounted for in a database which will be supplied with the software. The database is condensed from laboratory measurements and computer simulations of detector performance, and will be updated as the mission progresses. Depending on the user's preferences (and with intelligent defaults), the software will use the various parts of this database to create a response matrix appropriate for each observation.

When the user is only interested in isolated gamma-ray lines, the response is just the efficiency for photopeak detection, and the conversion from counts to photons is done immediately by dividing by the efficiency. This will also be adequate for hard x-ray flares with no significant component above 100 keV, since the response of the front segments below this point is dominated by complete absorption, not scattering.

Often, however, the desire will be to correct the entire spectrum, lines and continuum, over a broad energy range. In this case, the usual procedure will be to specify a model form of the spectrum, which can be a combination of either simple functions (power laws, Gaussians, etc.) or physics-based spectral forms (e.g. a set of known nuclear lines from a particular element bombarded by energetic protons, or a thin-target bremsstrahlung spectrum from a monoenergetic electron beam). The software will then "fold" this spectrum through the response matrix, check the goodness of fit to the observed count spectrum, and repeat the process, varying the parameters of the input model until the best fit is found. The output of this process is either the best-fit parameters themselves, or else a spectrum created by multiplying the observed count spectrum by the ratio of the model photon spectrum to the model count spectrum.

The HESSI software will include code that performs this iterative fitting, but we will also provide tools to export the count spectrum and response matrix to the XSPEC package (Arnaud 1996). XSPEC has a wider variety of built-in spectral models than will be available with HESSI. In addition, later versions of the HESSI software will have an algorithm for model-independent inversion of the spectra (Johns & Lin 1992; Smith et al. 1995). This algorithm will probably be most useful for spectra which are dominated by the continuum, not lines, but which extend to high enough energies that simply dividing by the efficiency is insufficiently accurate.

Armed with (mostly) instrument-independent spectra, the scientist will be ready to search for spectral signatures of elemental abundances, bremsstrahlung processes, directionality of proton beams, and all the other effects discussed in this volume.

Acknowledgments. The authors would like to thank our commercial partner, PerkinElmer Instruments, who produced the HESSI germanium detectors, and to note the efficiency and creativity of Dr. Thomas W. Raudorf and the detector processing group. We would also like to thank Dr. Stephen Castles, Robert Boyle, and ??? of the Goddard cryogenics group for providing and supporting the cryocooler and associated systems. Finally, we would like to thank our colleagues at the Space Sciences Laboratory: the technicians, machinists, and others who helped build the HESSI spectrometer.

References

Arnaud, K. 1996, Astronomical Data Analysis Software and Systems V, eds. Jacoby G. and Barnes J., ASP Conf. Series 101, 17

Hull, E. L. 1998, Ph.D. dissertation, Indiana University

Johns, C. M., & Lin, R. P. 1992, Solar Phys. 137, 121 (Erratum: Solar Phys., 142, 219)

Koenen, M. et al. 1995, IEEE Trans. Nucl. Sci. 42, 653

Landis, D. A., Cork, C. P., Madden, N. W., & Goulding, F. S. 1981, Presented at the IEEE Nucl. Sci. Symp., San Francisco, 21-23 Oct. 1981

Smith, D. M. et al. 1995, J. Geophys. Res., 100, 19675

Smith, D. M. et al. 2000, in AIP Conf. Proc., The 5th Compton Symposium, (New York: AIP), in press